Journal of Food Engineering 150 (2015) 99–105

Contents lists available at ScienceDirect

Journal of Food Engineering

journal homepage: www.elsevier.com/locate/jfoodeng

Effect of changes in microwave frequency on heating patterns of foods in a microwave assisted thermal sterilization system

F.P. Resurreccion Jr. [b], D. Luan [a], J. Tang [a,*], F. Liu [a], Z. Tang [a], P.D. Pedrow [c], R. Cavalieri [d]

[a] Biological Systems Engineering Department, Washington State University, Pullman, WA 99164, USA
[b] Graphic Packaging International, Inc., 4455 Table Mountain Drive, Golden, CO 80403, USA
[c] School of Electrical Engineering and Computer Science, Washington State University, Pullman, WA 99164, USA
[d] Agricultural Research Center, College of Agricultural, Human, and Natural Resource Sciences, Washington State University, Pullman, WA 99164, USA

ARTICLE INFO

Article history:
Received 20 May 2014
Received in revised form 22 September 2014
Accepted 1 October 2014
Available online 4 November 2014

Keywords:
Microwave heating
Computer simulation
Frequency shift
Dielectric property
Heating pattern

ABSTRACT

This research studied the influence of frequency variation on heating patterns within prepackaged foods in a 915 MHz single-mode microwave assisted sterilization (MATS) system consisting of four microwave heating cavities. The frequencies of the four generators powering the MATS system at Washington State University were measured at different power levels over one year. The effect of frequency shifts in the generators on heating patterns within a model food (whey protein gel, WPG) was studied through computer simulation. The simulated heating patterns were experimentally validated using a chemical marker. Our measurement results showed that a 0.5 kW increase in the microwave power caused the operating frequencies of the generators to increase by 0.25–0.75 MHz. The simulation results suggested that the heating pattern of WPG processed by the MATS system was not affected by the varying frequencies of generators within the operating frequency bandwidth (900–920 MHz). In addition, the simulation results revealed that using deionized water as the circulation medium in the MATS system resulted in a 23–37% increase in the temperature of WPG as compared with that when using normal tap water, but did not alter the heating pattern.

1. Introduction

The Federal Communications Commission (FCC) of the United States designated 915 ± 13 MHz and 2450 ± 50 MHz for industrial, scientific, and medical uses other than telecommunications. However, the operating peak frequency of a magnetron may vary within or beyond the allocated bandwidth. The variations are caused by differences in design and manufacture of magnetrons and the generators. A magnetron may also experience frequency shifts as it ages (Cooper, 2009). An important reason for the frequency shift would be the reduction of strength of the permanent magnet in the magnetron (Decareau, 1985). Finally, the operating frequency of a microwave generator also changes with the power setting during operation.

The heating pattern of food in a microwave heating system is determined by the microwave propagations and resonant modes within the microwave heating cavities. Each mode has a matched frequency. In a multimode microwave heating cavity with fixed dimension, the mode type is determined by the microwave frequency. A small shift in frequency may result in a different mode type (Dibben, 2001), which can lead to unpredictable heating patterns. For industrial microwave assisted thermal processes that require regulatory acceptance for food safety purposes, it is highly desirable that the systems provide predictable and repeatable heating patterns in the processed foods to allow accurate monitoring of temperature history at the cold spots. A 915 MHz single mode microwave assisted thermal sterilization (MATS) system was developed at Washington State University (WSU) with the ultimate goal for industrial implementation (Tang et al., 2006). The MATS system was powered by four high-power magnetron generators. Since its inception, several MATS processes for different foods in either rigid trays or flexible pouches were developed by the WSU research team and accepted by the United States Food and Drug Administration (FDA) or the United States Department of Agriculture Food Safety and Inspection Service (USDA, FSIS). After monitoring the operating frequencies of the four generators of the MATS system over one year (2009–2010), we noticed changes in their peak frequencies. Although no change in the heating patterns were observed during microwave processing, it is necessary to systematically investigate the effect of the operation peak frequency on microwave heating of foods and determine the

* Corresponding author.
E-mail address: jtang@wsu.edu (J. Tang).

http://dx.doi.org/10.1016/j.jfoodeng.2014.10.002
0260-8774/

frequency boundaries of the current system design without causing a change in the heating pattern. Such information is needed to guide future development of system operation and calibration protocols that assure consistent industrial production of safe foods using the MATS systems. Computer simulation was used in this study to systematically evaluate the limits for microwave operation frequency shift that would not potentially alter heating patterns during thermal processing in the WSU MATS system and guide future design and operations of similar industrial systems.

Microwave heating systems have been modeled using various numerical methods including the Finite Difference Time Domain (FDTD) method (Sundberg et al., 1996; Chen et al., 2008) and Finite Element Method (Zhou et al., 1995; Romano et al., 2005; Hossan et al., 2010). A typical assumption of such simulation models considered that microwave energy was transmitted at a fixed operating frequency. No study was conducted to quantify the effect of frequency shift of microwave on food heating patterns.

Therefore, the objectives of this study were to evaluate the factors responsible for possible changes in the peak frequency of microwave generators and determine the boundary of the frequency shift to ensure that no change in heating patterns would occur during microwave heating using the MATS and similar systems.

2. Materials and methods

2.1. MATS system

The MATS system developed and installed at WSU was used in this study (Resurreccion et al., 2013). It consisted of four sections, i.e., preheating, heating, holding and cooling, arranged in series representing the four sequential processing steps. In operation, the system was pressurized while the circulating water in each section was set at a certain temperature. A pocketed mesh conveyor belt made of non-metallic material extending from the start of the preheating section to the end of the cooling section conveyed the food trays or pouches through the MATS system.

This study was primarily concerned with general heating patterns in pre-packaged food in the microwave heating section of the MATS system. The microwave heating section consisted of four connected rectangular cavities. The cavities were specially designed to operate in single mode (*i.e.*, only one pattern of electromagnetic field distribution in each cavity) (Tang et al., 2006). Each cavity (Fig. 1) had two windows (top and bottom) made of high temperature resistant polymer. The microwaves were delivered to the cavity through the windows that were connected to two horn microwave applicators. The horn was a tapered shape with the wide end connected to the window and the narrow end having the same inner cross sectional dimension as that of a standard WR975 waveguide (247.7 mm by 123.8 mm). The microwaves were directed from generators to the horn applicators through WR975 rectangular waveguides consisting of six 90° E-bend waveguide elbows, a 90° H-bend waveguide elbow, and a tee junction. Incident microwaves were bifurcated at the tee junction wherein two equal portions propagating to the top and bottom horns and merging in the cavity without phase shift. In the MATS system, cavity 1, 2, 3, and 4 were connected to generator 1, 2, 3, and 4, respectively.

2.2. Computer simulation model for the MATS system

The geometry and dimension of the microwave heating section, including the heating cavities and horn applicators, was incorporated in computer simulation model (Fig. 2). Since a pseudo location for microwave input port can be drawn anywhere within the waveguide (*i.e.*, as long as it is parallel to the cross section of the waveguide), port locations were selected just above and below the narrow ends of the horns (Fig. 2a). The selected location of microwave input ports allowed for the exclusion of the waveguides connecting the applicators to the microwave generators. Doing so could reduce the dimension of the simulation model and minimize the computational resources.

The power setting of each port was based on the net output power of each generator. The generator output powers were measured by directional couplers (Ferrite Microwave Technologies, Inc., Nashua, NH 03060) installed along the waveguides through an automated feedback mechanism. The power settings of the four microwave heating cavities were 6.4, 5.6, 2.5, 2.6 kW, respectively. In the simulation model, the net input power of each cavity was evenly distributed to the two ports.

The finite difference time domain (FDTD) method was used to numerically solve the coupled electromagnetic and heat transfer equations during microwave processing. The simulation was conducted using a commercial software of Quickwave version 7.5 64-bit (QWED, Warsaw, Poland). The FDTD cell size in this study was 4, 4 and 1 mm in x, y, and z direction (Fig. 2), respectively. It followed a general rule by thumb that the discrete cell dimension

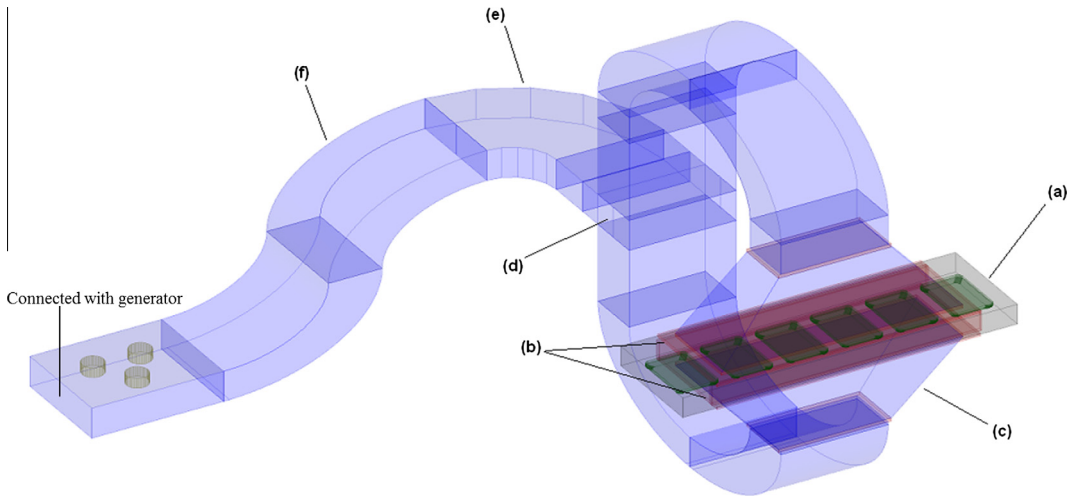

Fig. 1. A typical microwave heating cavity and its attachments of the MATS system. (a) A single mode cavity, (b) two microwave transparent windows at the top and bottom of the cavity, (c) one of the two horns at bottom, (d) a tee waveguide junction, (e) a 90° H-bend waveguide elbow, (f) one of the six 90° E-bend waveguide elbow.

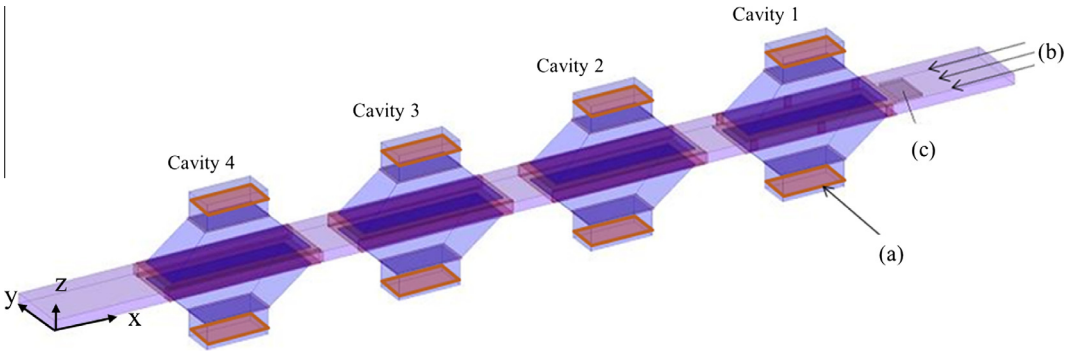

Fig. 2. Computer simulation model for microwave heating section consisting of four heating cavities and eight horn applicators. (a) Location of microwave input ports (eight ports in the model), (b) direction of movement of pouches, (c) location of the food pouches.

should be less than one tenth of a wavelength (Rattanadecho, 2006). Mesh refinement was made on the edge of the food in both *x* and *y* directions. The mesh refinement covered 30 mm of the four sides of the food in *x*–*y* plane, refining the mesh size to 3 mm. Details of the computer simulation model for MATS including pertinent equations and boundary conditions were discussed in Resurreccion et al. (2013).

In this study, whey protein gel (WPG) (Lau et al., 2003) was used as the model food for experimental verification of the heating pattern generated by the computer simulation model. The dimension of the WPG used in this study was $84 \times 127 \times 16$ mm^3 (*i.e.*, *x*, *y*, *z*). The mean values of dielectric and thermal properties in Table 1 of WPG were used in the computer simulation model. In the actual operation of the MATS system, the belt that held the WPG in pouches moved at a speed of approximately 17 mm/s along the *x*–*y* plane in the direction illustrated in Fig. 2b. Considering the 3094 mm combined length of the four cavities, the belt movement would translate into 182 s total microwave heating time. To incorporate WPG movement in the simulation model, the total length of the four cavities was discretized into 32 steps wherein each step length was 3094 mm/32 or 96.67 mm, and each step had a heating time of 182 s/32 or 5.69 s. The heating pattern inside the WPG at the end of the 32nd step was analyzed.

2.3. Frequency measurement

The microwave generators for the first and second cavities were manufactured by Ferrite Microwave, Inc (Nashua, NH 03060), and those for the third and fourth cavities by Microdry Industries, LLC (Crestwood, KY 40014). A TM-2650 spectrum analyzer and an AN-301 antenna (B&K Precision, Yorba Linda, CA) were used to measure the frequencies of the generators. Frequency measurements were carried out using the direct method described in ITU (2003).

The AN-301 is a dipole antenna specified to work at a frequency range of 0.8–1.0 GHz. It has a gain equal to or greater than +1 dBi, and a voltage standing wave ratio equal to or less than 1.5 at the center of the frequency range. Fig. 3 illustrates a typical measurement using the instrument that shows the location of the peak or operating frequency and the corresponding value. The TM-2650 spectrum analyzer was set to a central frequency of 915 MHz with a span of 200 MHz (*i.e.*, from 815 MHz to 1015 MHz on the *x*-axis). The frequency span was subdivided into 10 divisions, and each division was 20 MHz. The oscillation power was set to −60 to 0 dBm (decibel relative to one milliwatt) on the *y*-axis subdivided into 6 divisions, and each division was 10 dBm. The occupied frequency bandwidth (OFBW) was measured by considering 80% of the total measured power.

The peak frequency (*i.e.*, nominal frequency) and the OFBW were measured for the first and second microwave generators with power settings from 2 kW to 10 kW with 0.5 kW increments. For the third and fourth microwave generators, the peak frequency and OFBW were measured from 0.5 kW to 4.7 kW with 0.5 kW increments. All the frequency measurements were done in three replicates every other month for a period of one year.

2.4. Simulation cases at different operating frequencies

Different simulation cases were conducted covering the possible operating frequency range of 900–920 MHz (Table 2) to study the effect of frequency shift on the heating pattern of food. Cases 1–5 were ideal scenarios in which all the generators were set at the same frequency. The operating frequency used for Case 1 was 900 MHz, and incremented by 5 MHz for each of the next case. Case 6 was a simulation emulating a real case scenario (*e.g.*, actual power setting in Table 3 and the corresponding measured operating frequency of the four generators).

Another factor that may affect the heating process was the loss factor of the circulating hot water (122 °C) inside the microwave heating cavities. When the loss factor was relatively high (*e.g.*, for tap water), the water acted as a lossy material absorbing microwave energy which would lead to a moderate heating rate of food. On the contrary, the deionized water, which has a lower loss factor, may increase the heating rate of the food. To quantify the effect of the different loss factors of water, the simulation runs were conducted following the design in Table 3 using both the loss factor of tap water, $\varepsilon_r'' = 2.70$ at 122 °C and 915 MHz (Komarov and Tang, 2004), and that of deionized water, $\varepsilon_r'' = 1.35$ at 122 °C and 915 MHz (measured using a Hewlett–Packard™ 8752C network analyzer).

Table 1
Dielectric and thermal properties of whey protein gel.

Temperature (°C)	Relative dielectric constant (ε_r')	Relative loss factor (ε_r'')	Specific heat (c_p) (J/(g °C))	Thermal conductivity (k) (W/(m °C))
20	23.58 ± 2.75	52.91 ± 2.49	–	–
40	29.26 ± 1.01	51.76 ± 0.99	–	–
60	34.85 ± 1.53	50.62 ± 0.77	3.15 ± 0.13	0.52 ± 0.03
80	41.68 ± 1.97	49.35 ± 1.45	3.41 ± 0.02	0.53 ± 0.02
100	50.73 ± 1.74	48.11 ± 1.74	3.63 ± 0.03	0.55 ± 0.01
120	58.40 ± 3.02	47.42 ± 1.15	3.66 ± 0.16	0.55 ± 0.03

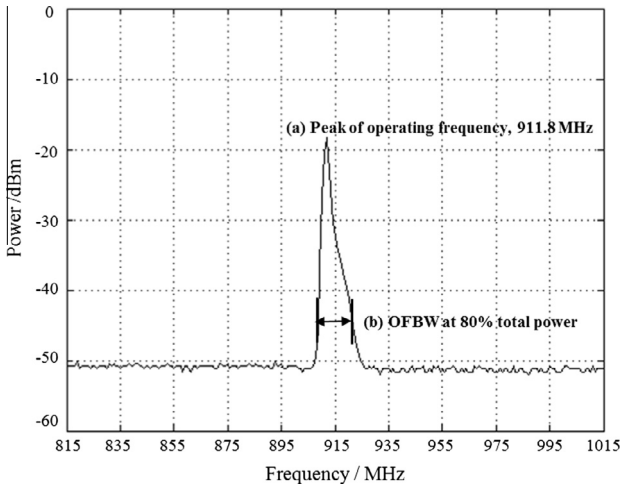

Fig. 3. A typical result of frequency measurement. (a) Peak or operating frequency, (b) occupied frequency bandwidth (OFBW) at 80% total power.

Table 2
Frequency settings of each simulation case.

Simulation case	Frequency settings on four generators
Case 1	900 MHz
Case 2	905 MHz
Case 3	910 MHz
Case 4	915 MHz
Case 5	920 MHz
Case 6	Actual operating frequency[a]

[a] The measured frequency of the transmitted power on every cavity was listed in Table 3.

Table 3
Measured operating frequency for the typical power setting of microwave generators.

Microwave generator	Transmitted microwave power (kW)	Operating frequency (MHz)[a]	OFBW at 80% total power expressed as deviation (MHz)
Generator 1	6.40	912.08	±3.79
Generator 2	5.56	916.58	±4.18
Generator 3	2.51	905.62	±3.68
Generator 4	2.59	903.09	±4.25

[a] Frequency used for Case 6 simulation in Table 2.

2.5. WPG as a model food and its physical property measurement

Preparation of WPG was described in the study of Pandit et al. (2006, 2007). The dimension of the WPG used in this study was $84 \times 127 \times 16\ mm^3$ (*i.e.*, *x*, *y*, *z*); the WPG was packed in an 8-oz. flexible pouch with a dimension of $95 \times 140\ mm^2$ (*i.e.*, *x*, *y*). PrintPack® pouches designed for the MATS application were used.

A Hewlett–Packard™ 8752C network analyzer was used to measure the dielectric properties of the WPG following the procedure described in Wang et al. (2008). Specific heat and thermal conductivity were measured through with the double needle method (Campbell et al., 1991) using Decagon™ KD2-pro (Decagon, WA, USA). The density of WPG is approximately equal to $1.0\ g/cm^3$ following the method described by Krokida and Maroulis (1997).

2.6. Processing of WPG in MATS system

Pouches of WPG were loaded on the conveyor belt through the door and moved to the preheating section of the MATS system. Then the door was closed and the system was pressurized to 234 kPa (gauge). The circulating water (50–55 L/min) were pumped into preheating, heating, holding and cooling sections with preset temperatures of 72 °C, 122 °C, 122 °C and 20 °C, respectively. After 30 min preheating, food pouches were transported through microwave heating, holding section and finally moved to the cooling section at a constant speed of 17 mm/s. The WPG inside the pouches was cooled in the cooling section for 5 min before retrieving.

In the preheating section, the temperature of the food was allowed to equilibrate to a uniform initial temperature. As food trays or pouches traversed the microwave heating section, food was heated by the combination of the thermal energy from the circulating hot water and the microwave energy from the four applicators connected to the microwave generators. The nominal operating frequency of the microwave generators was 915 MHz. The holding section following the microwave heating section provided the necessary residence time for the food to reach the desired sterilization value (F_0). The packaged foods finally entered the cooling section for rapidly cooling to 20 °C. After cooling, the heating pattern of the processed WPG was obtained through a computer vision method (Pandit et al., 2007). Six samples of WPG were used for this purpose.

2.7. Chemical marker based computer vision method

Chemical marker M-2 was a product of the non-enzymatic browning reaction between D-ribose and amines (*i.e.*, both present in the WPG formulation) when the temperature was over 100 °C. The production of M-2 was an irreversible process and was dependent on accumulated effect of heat treatments. Furthermore, M-2 was brown in color and the intensity of the brownness was directly proportional to the amount of produced M-2 (Pandit et al., 2006). Different intensities of brown color at different locations in the WPG allowed for a qualitative determination of the heating pattern.

The original heating pattern was processed by the computer vision method to create colorful heating patterns. In the computer vision system, two standards were used as a basis for the lightest brown and the most intense brown colors. The lightest brown was based on the color of unprocessed WPG, and the most intense brown was based on the overheated WPG (with saturated brown color). The RGB values which describe the final heating patterns were then scaled based on the two standards. The detailed procedure for determining the heating pattern in the RGB scale was described in by Pandit et al. (2007).

3. Results and discussion

3.1. Frequencies at different power levels

Fig. 4 summarizes the measured peak or operating frequencies (Fig. 3a) of the four generators at different power settings. The data represent the averages of six measurements done every other month for a period of one year. The standard deviation shows the frequency shift of each generator in one year.

Generators 1 and 2 manufactured by Ferrite™ had varying operating frequencies typically within 1–2 MHz over one year for a specific power setting. Considering the 2–10 kW possible power settings for generators 1 and 2, the operating frequency bandwidth of generators 1 and 2 was 908–914 MHz and 912–919 MHz, respectively. In comparison, generators 3 and 4 manufactured by Microdry™ had relatively consistent operating frequencies (<1 MHz variation) during one year period. No significant operating frequency shifting was observed at higher power settings (>2 kW).

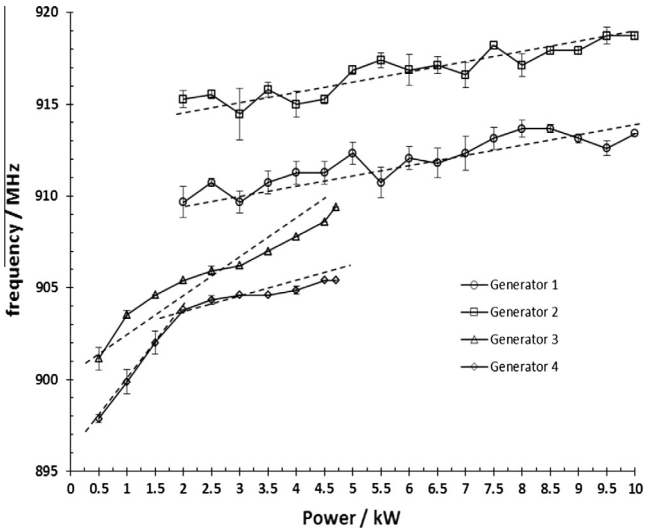

Fig. 4. Plot of operating frequency versus power setting of each generator. Six measurements at each power setting were carried out every other month for a period of one year (2009–2010).

Considering the 1–4.7 kW possible power settings for generators 3 and 4, the operating frequency bandwidth for generators 3 and 4 was 901–909 MHz and 898–905 MHz, respectively. The consistency of generators from operating at a certain frequency might be related to the differences in the designs and components of the magnetrons of the generators.

In general, the operating frequency was directly proportional to the power setting (*i.e.*, the higher the power setting of the generator, the higher the operating frequency). With generators 1 and 2, for every 0.5 kW increase in power, the operating frequency increased by 0.25 MHz. At the same power setting, generator 2, on average, operated at 4.8 MHz higher than generator 1. For generator 3 and 4, the operating frequency was increased by 0.75 MHz for every 0.5 kW increase in the power setting. Also, at the same power setting, generator 3, on average, operated 2.7 MHz higher than generator 4.

Although a general trend between operating frequency and power setting has been established, generators manufactured by Ferrite™ (Model GET-2024) are less consistent in achieving a certain value of operating frequency than those manufactured by Microdry™ (Model IV-74) (Fig. 4). Generators 1 and 2 (*i.e.*, Ferrite™) produced an up and down trend of operating frequency with power and a relative high standard deviation (*i.e.*, approximately ±1 MHz) among measurement trials. For generators 3 and 4 (*i.e.*, Microdry™), the curve was relatively smooth and the standard deviation among trials was much lower (*i.e.*, approximately ±0.3 MHz). A possible explanation was that the Ferrite™ generators were originally designed to operate at a full power of 75 kW. But they were modified to operate at much lower power (15 kW) needed for WSU MATS system.

The occupied frequency bandwidth (OFBW), however, seems to be independent from the power setting of the generator. When looking at 80% of the total power measured by the spectrum analyzer, the average OFBWs for generators 1, 2, 3, and 4 were 7.58, 8.35, 7.36, and 8.50 MHz, respectively.

3.2. Frequencies at operation power settings

Generators 1 and 2 were relatively close to the FCC allocated mean frequency of 915 MHz, but generator 3 and 4 were slightly lower (Fig. 4). This might be due to the differences in the design and the age of the generators. Generators 1 and 2 (built in 2008) were relatively newer than generators 3 (built in 1991) and 4 (built in 1996). Furthermore, considering the OFBW at 80% total power of the generators, the measured operating frequencies in Table 3 were within the experimental design in Table 2. The chosen 900–920 MHz range of frequency roughly covered the lowest and highest possible operating frequencies of the generators.

3.3. Heating pattern validation through chemical marker method

Fig. 5 shows that the heating pattern generated from computer simulation (Case 6) is comparable to the heating pattern identified through the chemical marker method using WPG as the model food. Both images were on the *x*–*y* plane and in the middle with respect to the sample's thickness (*i.e.*, *z* axis). The heating pattern was symmetrical in the *x*–*y* plane and can be summarized into three areas: Cold Area 1, Cold Area 2, and Hot Area (Resurreccion et al., 2013). The temperature distribution within a given area was relatively uniform. The top and bottom areas in *y* direction were at a lower temperature and qualitatively described by the green/bluish color, corresponding to Cold Area 1. The central area was also at a lower temperature which corresponds to Cold Area 2. The areas above and below Cold Area 2 qualitatively described by the red color corresponds to the Hot Area. The heating pattern of experimental result was correctly predicted by computer simulation. The validated simulation model will be applied to study the

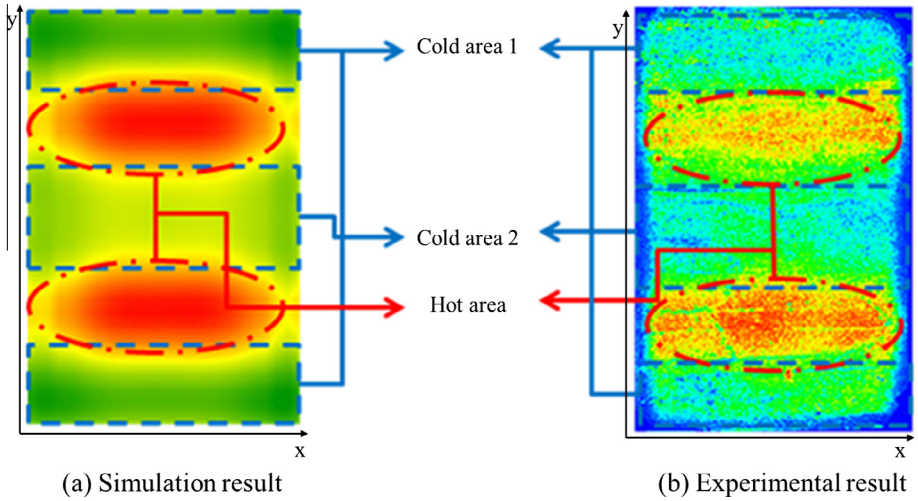

Fig. 5. Comparison of heating patterns. (a) Simulation result (Case 6), (b) experimental result from chemical marker method (from Resurreccion et al., 2013).

influence of frequency shifts on heating pattern of food processed in MATS system. However, the simulation results overestimated temperature rises during the thermal processes within the MATS system. Thus, in this study our main interest in using this model was the prediction of heating patterns.

3.4. Influence of frequency shifts on heating patterns

The simulation results of the heating patterns in the *x*–*y* plane at the middle layer (*z* direction) of the sample are summarized in Fig. 6. The general heating pattern was not affected by frequency shift of the microwave generator within the range of 900–920 MHz. However, the temperature (*i.e.*, associated to heating rate) increased with an increase in frequency. The difference in overall sample temperature at different frequencies was most significant at the exit of the second cavity (Fig. 6a-iii and b-iii).

At lower frequency (*e.g.*, Case 1 at 900 MHz), there was a clear distinction between cold and hot areas. But at a higher frequency (*e.g.*, Case 5 at 920 MHz), the hot areas expanded. At 900 MHz, in Fig. 6a – Case 1, the cold area between two hot areas is mostly green, corresponding to a temperature range of 110–112 °C; and in Fig. 6b – Case1, the cold area is red corresponding to a temperature range of 170–180 °C. However, at 920 MHz in Fig. 6a – Case 5, the cold spot area between two hot areas is mostly yellow corresponding to a temperature of about 120 °C; and in Fig. 6b – Case 5, everything is pink which corresponds to a temperature >200 °C. Dissipation of microwave power into heat was higher at higher frequency causing the sample to increase in temperature, the hot areas to occupy a bigger region, and the cold area sandwiched between the two hot areas to be a reduced region (Incropera et al., 2007). As stated earlier, the simulation model used in this study over-estimated sample temperatures (Resurreccion et al., 2013). Thus, the above discussion of sample temperatures only helped to compare relative heating intensities of different simulated cases.

In Case 6 which simulates the process with actual operating frequencies (Tables 2 and 3), the final heating pattern was similar to the result between those of the simulation for Case 3 and Case 4 (Fig. 6). Although the average frequency for Case 6 is 909.34 MHz which fell between Case 2 and Case 3 (*i.e.*, 905 MHz and 910 MHz, respectively), generator 1 and generator 2 were operat-

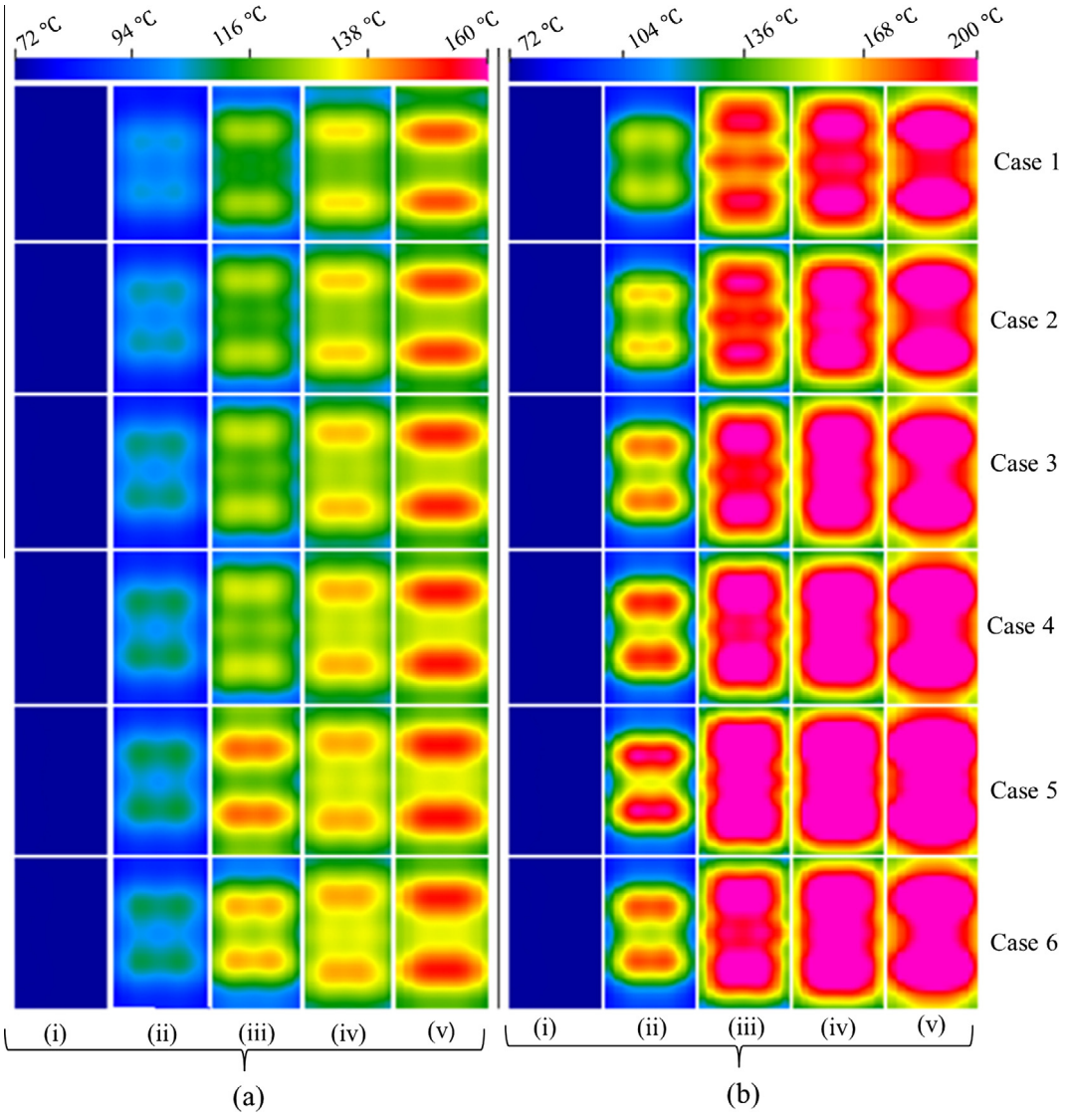

Fig. 6. Heating pattern snapshot in the middle layer for package WPGs in the six simulation cases. (a) Simulation result for sample in tap water ($\varepsilon_r'' = 2.70$ at 122 °C and 915 MHz), (b) simulation result of sample in deionized water ($\varepsilon_r'' = 1.35$ at 122 °C and 915 MHz). The temperature scale gradient is 72–160 °C for (a) and 72–200 °C for (b). Column (i) is the initial heating pattern, and columns (ii), (iii), (iv), and (v) are heating patterns at the exit of first, second, third, and forth cavity, respectively.

ing at higher frequencies and powers (Table 3), and should therefore have a larger contribution to heating pattern.

Comparing group (a) and group (b) in Fig. 6, the loss factor of the circulating water inside the cavity had a significant influence on the intensity of temperature in the sample. Although the patterns were similar for both groups, reducing the loss factor of circulating water by half (from $\varepsilon_r'' = 2.70$ for tap water to $\varepsilon_r'' = 1.35$ for deionized water) would result in a 23–37% increase in temperature. The reason was that the amount of microwave energy dissipated to heat is different in different circulating waters. For higher lossy circulating water such as tap water, a relatively large amount of the microwave energy was absorbed by the water reducing the amount of energy that may be absorbed by the food. For relatively lower lossy water such as deionized water, less microwave energy was absorbed by the circulating water. This made most of the incident microwave energy available to food material, producing higher heating rate and final temperature of the food. In actual processing in the MATS system, during the application of microwave power to the heating cavities, there is an average of 2–3 °C increase in temperature of the circulating water (*i.e.*, from 122 °C to 124–125 °C) showing that water indeed absorbed microwave energy. The microwave energy absorbed by the water is then subsequently taken off by the chilling water through a heat exchanger attached to the MATS system, which then reduces the temperature back to 122 °C before entering the microwave heating section.

4. Conclusions

From above discussion, the following conclusions could be derived:

- The operating frequencies of four generators powering the MATS system were influenced by the power settings. Every 0.5 kW increase in power caused an operating frequency increase by a 0.25 MHz for generators 1 and 2, and by 0.75 MHz for generators 3 and 4. However, within a period of one year there was no significant frequency shift for each generator at a fixed power setting.
- Both the simulation and the chemical marker method suggested that the heating pattern was symmetrical in *x*–*y* plane and could be summarized into three areas (*i.e.*, Cold Area 1, Cold Area 2, and Hot Area). The temperature distribution within a given area was relatively uniform.
- The operating frequency of the microwave generators ranged from 900 MHz to 920 MHz did not affect the heating pattern inside the food. But higher operating frequency resulted in an increase of food temperature.
- The overall effect of reducing the loss factor of circulating water in the microwave heating cavities was an increase in temperature of the food. Compared with tap water, using deionized water as the circulating water caused a 23–37% increase in the overall temperature of WPG.

Acknowledgements

We acknowledge the support of the Agriculture and Food research Initiative of the USDA National Institute of Food and Agriculture, grant number #2011-68003-20096 and Agriculture Research center of Washington State University. The authors also thank the Chinese Scholarship Council for providing a scholarship to Donglei Luan for his Ph.D. studies.

References

Campbell, G.S., Calissendorff, C., Williams, J.H., 1991. Probe for measuring soil specific-heat using a heat-pulse method. Soil Sci. Soc. Am. J. 55 (1), 291–293.
Chen, H., Tang, J., Liu, F., 2008. Simulation model for moving food packages in microwave heating processes using conformal FDTD method. J. Food Eng. 88 (3), 294–305.
Cooper, N., 2009. Microwave Oven. In: Lorence, M.W., Pesheck, P.S. (Eds.), Development of Packaging and Products for Use in Microwave Ovens. CRC Press LLC, Boca Raton, pp. 105–127.
Decareau, R.V., 1985. Microwaves in the food processing industry. Academic Press Inc., Orlando, FL, USA.
Dibben, D., 2001. Electromagnetics: fundamental aspects and numerical modeling. In: Datta, A.K., Anantheswaran, R.C. (Eds.), Handbook of Microwave Technology for Food Applications. CRC press, Boca Raton, FL, pp. 1–28.
Hossan, M.R., Byun, D., Dutta, P., 2010. Analysis of microwave heating for cylindrical shaped objects. Int. J. Heat Mass Transf. 53 (23–24), 5129–5138.
Incropera, F.P., Dewitt, D.P., Bergman, T.L., Lavine, A.S., 2007. Introduction to heat transfer, 5th ed. John Wiley & Sons Inc., Hoboken, NJ, USA.
ITU, 2003. Techniques for Measurement of Unwanted Emissions of Radar Systems (ITU document WP8B ITU-R M1177). International Telecommunication Union (ITU).
Komarov, V.V., Tang, J., 2004. Dielectric permittivity and loss factor of tap water at 915 MHz. Microw. Opt. Technol. Lett. 42 (5), 419–420.
Krokida, M.K., Maroulis, Z.B., 1997. Effect of drying method on shrinkage and porosity. Drying Technol. 15 (10), 2441–2458.
Lau, M.H., Tang, J., Taub, I.A., Yang, T.C.S., Edwards, C.G., Mao, R., 2003. Kinetics of chemical marker formation in whey protein gels for studying microwave sterilization. J. Food Eng. 60, 397–405.
Pandit, R.B., Tang, J., Mikhaylenko, G., Liu, F., 2006. Kinetics of chemical marker M-2 formation in mashed potato – a tool to locate cold spots under microwave sterilization. J. Food Eng. 76 (3), 353–361.
Pandit, R.B., Tang, J., Liu, F., Mikhaylenko, G., 2007. A computer vision method to locate cold spots in foods in microwave sterilization processes. Pattern Recogn. 40 (12), 3667–3676.
Rattanadecho, P., 2006. The simulation of microwave heating of wood using a rectangular wave guide: influence of frequency and sample size. Chem. Eng. Sci. 61, 4798–4811.
Resurreccion, F.P., Tang, J., Pedrow, P.D., Cavalieri, R., Liu, F., Tang, Z., 2013. Development of a computer simulation model for processing food in a microwave assisted thermal sterilization (MATS) system. J. Food Eng. 118 (2013), 406–416.
Romano, V.R., Marra, F., Tammaro, U., 2005. Modelling of microwave heating of foodstuff: study on the influence of sample dimensions with a FEM approach. J. Food Eng. 71 (3), 233–241.
Sundberg, M., Risma, P.O., Kildal, P.S., Ohlson, T., 1996. Analysis and design of industrial microwave ovens using the finite difference time domain method. J. Microw. Power Electromagn. Energy. 31 (3), 142–157.
Tang, J., Liu, F., Pathak, S., Eves, G., 2006. Apparatus and Method for Heating Objects with Microwaves, US Patent No. 7,119,313.
Wang, Y., Tang, J., Rasco, B., Kong, F., Wang, S., 2008. Dielectric properties of salmon fillet as a function of temperature and composition. J. Food Eng. 87, 236–246.
Zhou, L., Puri, V.M., Anantheswaran, R.C., Yeh, G., 1995. Finte-element modeling of heat and mass-transfer in food materials during microwave heating – model development and validation. J. Food Eng. 25 (4), 509–529.